Analysis of a Symmetrical Swept Airfoil at Varying Sweep Angles in AVL (Athena Vortex Lattice)

Eric Qiu

Guggenheim School of Aerospace Engineering, Georgia Institute of Technology

AE 6015: Advanced Aerodynamics

Dr. Lakshmi N. Sankar

March 28, 2022

Introduction and Background

The report of interest focuses on the aerodynamic analyses of a given symmetrical swept airfoil across multiple sweep angles, given that the airfoil is neither tapered nor twisted. The approach method is the vortex lattice method using eight spanwise strips and five chordwise panels, with the control points located at 3/4th chord. The given aspect ratio for the airfoil is 5. The parameters of interest are found in Table 1. The results of interest are the induced drag polars, or the plot of $C_{d_i} vs. C_l$, as well as $C_l \ vs. \alpha$, or the lift-curve slope.

Note that due to the experimental set-up, the parameters in Table 1 produce five sets of resultant data, which will resolve into five separate drag polars (one for each sweep angle).

Table 1: Experimental airfoil parameters

Experimental Sweep Angles (deg)	Experimental Angles of Attack (deg)
0	2.1
15	4.2
30	6.3
45	8.4
60	10.5

The report applies the vortex lattice method (VLM) by using the open-source software AVL[1], otherwise known as Athena Vortex Lattice, written by Mark Drela and Harold Youngren. The vortex lattice method was explained in a previous assignment and thus the specifics will not be again described here. The program, written in FORTRAN, computes the induced drag coefficient and lift coefficient of swept wings under the following assumptions:

1. Viscous effects are negligible.

2. Turbulence, dissipation, and boundary layers are of negligible effect.

3. Flow is inviscid, incompressible, and irrotational.

4. Lifting surfaces are thin, or thickness influence on aerodynamic forces is negligible.

5. Angle of attack and sideslip angle are small.

Due to the implications of these assumptions, the AVL program is clearly incapable of handling such cases when any one or more of these assumptions do not hold true. With some modifications, specifically the 3-dimensional Prandtl-Glauert transformation, the program is capable of handling compressible subsonic flows to an extent, however this is not the intended purpose of AVL.

The results of this analysis were then compared against results from the USAF Stability and Control Digital DATCOM[2] (also written in FORTRAN), which is a far more complex program that takes in a .DAT file describing the geometry of an aircraft (or wing). For output, the DATCOM provides all the dimensionless stability derivatives of the input aircraft, as well as lift and drag coefficients. The DATCOM itself is a compilation of many proven methods, knowledge, and practices – in this sense, it is not at all akin to a modern CFD (computational fluid dynamics) approach, which finds more similarity with AVL (both are purely mathematical). For the purposes of this report, the lift-curve slope approximation obtained from the DATCOM is described in Equation 1.

$$Eq.1: C_{l_\alpha} = \frac{2 * \pi * AR}{2 + \sqrt{AR^2(1-M)^2\left(1 + \frac{\tan^2 \Lambda_{\frac{1}{2}}}{(1-M^2)}\right) + 4}}$$

where:

AR: The aspect ratio of the wing/airfoil

$\Lambda_{\frac{1}{2}}$: The mid-chord sweep angle (in this case, the same as the sweep angle anywhere else)

M: The Mach number (freestream)

Finally, the Weber & Brebner report[3] (referenced and described in Assignment 2) contains data on a similar airfoil, but only at a 45-degree sweep angle. Thus, the data from that specific case was similarly compared to the experimental results from that report.

Data Presentation and Discussion

The AVL results are shown in Tables 2-6. The experimental data from the Weber & Brebner report is appended in Table 6. The lift-curve slope plot appears in Figure 1. The induced drag polar plot appears in Figure 2. Table 7 compares AVL lift-curve slopes with DATCOM lift-curve slopes.

Table 2: AVL data for sweep angle of zero degrees

Angle of Attack (deg)	C_{d_i} @$\Lambda = 0°$	C_l @$\Lambda = 0°$
2.1	0.00278	0.31180
4.2	0.01108	0.62257
6.3	0.02479	0.93129
8.4	0.04373	1.23696
10.5	0.06763	1.53861

Table 3: AVL data for sweep angle of fifteen degrees

Angle of Attack (deg)	C_{d_i} @$\Lambda = 15°$	C_l @$\Lambda = 15°$
2.1	0.00265	0.29954
4.2	0.01055	0.59810
6.3	0.02360	0.89470
8.4	0.04162	1.18839
10.5	0.06438	1.47823

Table 4: AVL data for sweep angle of thirty degrees

Angle of Attack (deg)	C_{d_i} @$\Lambda = 30°$	C_l @$\Lambda = 30°$
2.1	0.00232	0.26294
4.2	0.00925	0.52502
6.3	0.02070	0.78538
8.4	0.03651	1.04318
10.5	0.05647	1.29760

Table 5: AVL data for sweep angle of forty-five degrees

Angle of Attack (deg)	C_{d_i} (AVL) $\Lambda = 45°$	C_l (AVL) $\Lambda = 45°$	$C_{d_i}(Weber\ \&\ Brebner)$ $\Lambda = 45°$	C_l $(Weber\ \&\ Brebner)$ $\Lambda = 45°$
2.1	0.00127	0.12721	---	0.121
4.2	0.00507	0.25396	0.005	0.238
6.3	0.01134	0.37982	0.012	0.350
8.4	0.02000	0.50435	0.022	0.456
10.5	0.03093	0.62711	0.035	0.559

Table 6: AVL data for sweep angle of sixty degrees

Angle of Attack (deg)	C_{d_i} @$\Lambda = 60°$	C_l @$\Lambda = 60°$
2.1	0.00052	0.05577
4.2	0.00207	0.11135
6.3	0.00463	0.16656
8.4	0.00817	0.22121
10.5	0.01263	0.27512

Generally, there appear to be a few notable trends among these data. First, the lift coefficient consistently increases with angle of attack, as expected based on knowledge of the interaction between angle of attack and lift coefficient at angles of attack below the stall point. Similarly, the drag coefficient exhibits the same phenomenon. Both values experience the largest change as angle of attack increases from 2.1 to 4.2 degrees, again lining up with expectations.

Now, sweep angle has the exact opposite effect – increasing sweep angle leads to a decrease in both drag and lift coefficients. The most significant change in lift curve slope occurs either between 45 and 60 degrees or 30 and 45 degrees of sweep angle (see Table 7 for further support) – it appears that, as sweep angle increases, the rate at which drag and lift coefficients decrease also increases.

This phenomenon can be explained simply. A swept wing meets the freestream airflow at an angle – thus, the flow can be resolved into two vectors (one parallel, one perpendicular) to the wing. With the assumptions from the previous section in place, the parallel vector has no impact on pressure distribution – the airflow is thus 'reduced' by a factor equivalent to the cosine of the sweep angle. That is, $C_l \sim cos\Lambda$, and it thus follows that $C_l' \sim (cos\Lambda)' = -sin\Lambda$. As the magnitude of sine increases with increasing angle of attack up to 90 degrees, this theoretical conclusion is in perfect agreement with the AVL results.

Comparing the results in Table 5 to the experimentally obtained data (also in Table 5), the AVL simulation is remarkably accurate, differing at most by about 6 or 7 percent. There could be many possible explanations for the inaccuracies, and these can be attributed to both sides. Inaccurate measurements are possible because the experimental data was measured in 1958. Similarly, AVL assumptions, most notably that angles of attack and sideslip are so small that sines of said angles are effectively zero, are likely not entirely justified. The mentioned assumption is likely the reason why the simulation grows less and less accurate as angle of attack increases. Regardless, the supplied and obtained data appear to agree.

It should be noted that all the above observations hold only when aspect ratio (AR) is held constant.

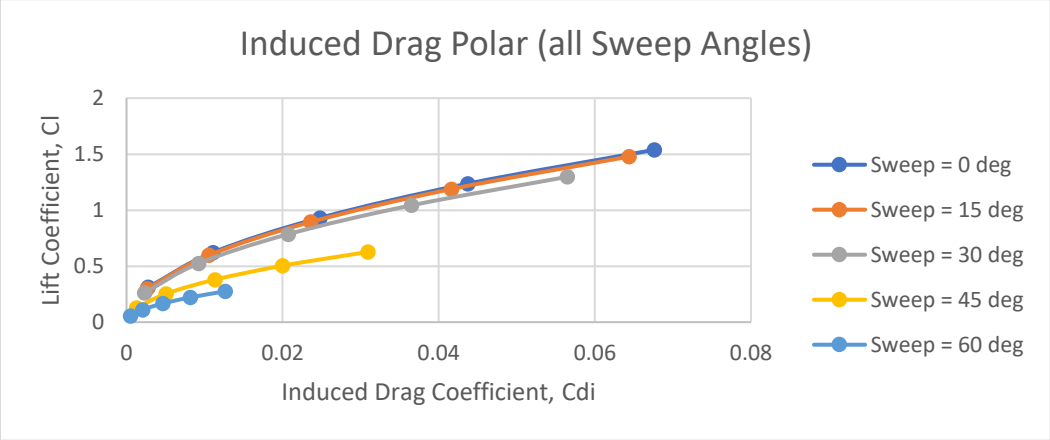

Figure 1

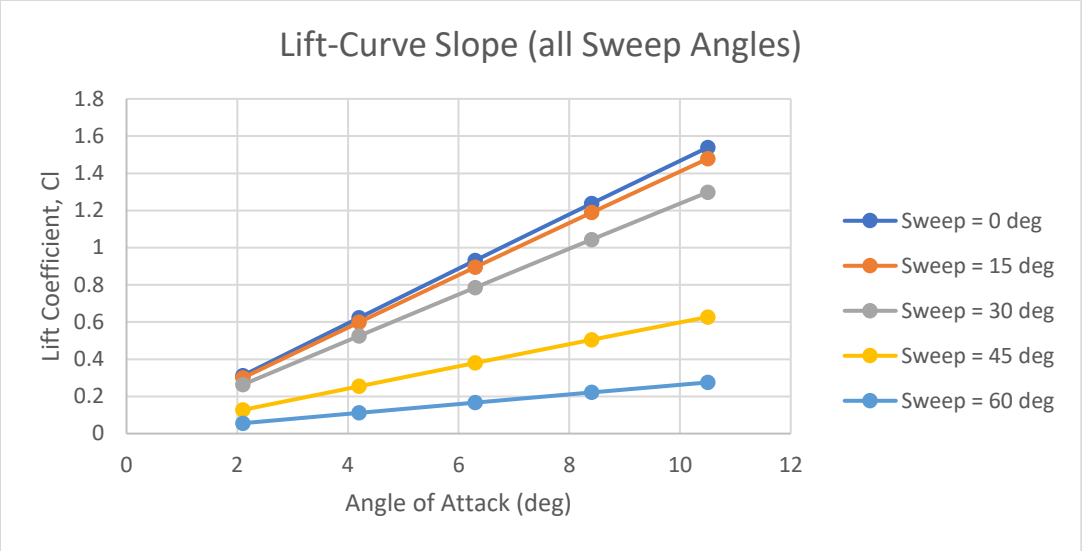

Figure 2

Table 7: AVL vs DATCOM data for lift-curve slopes, in 1/rad

Sweep Angle (deg)	$C_{l_\alpha}\ (DATCOM)$	$C_{l_\alpha}(AVL)$
0	4.253924	4.589867
15	4.161426	4.410796
30	3.873679	3.870442
45	3.360542	1.869248
60	2.575490	0.819956

Similarly, increasing the sweep angle allows for lower induced drag coefficients (Figure 1), but also decreases the coefficients of lift achievable at such low values of C_{d_i}, thus reducing the overall L/D ratio of the wing. This is mostly due to side-sweep effects – the air moving across the wing (parallel to it) increases the effect of the wing-tip vortices. The overall value of the induced drag coefficient still decreases but note that this is due to the induced drag depending on the square of the lift coefficient. A simple division (L/D ratio) will reveal that larger sweep angles negatively impact drag.

Finally, the lift-curve slopes (Figure 2) are compared to the DATCOM values in Table 7. The values differ rather significantly at higher angles of attack but are almost identical at lower angles of attack.. The previous explanation of the AVL small-angle assumption holding less and less true as angles increase is repeated here. There can be no other simple explanation besides that one of the AVL

assumptions must be flawed, as it is much less likely that the DATCOM, with its compilation of data, is the inaccurate of the two.

Conclusion

The main conclusions are that swept wings negatively impact wing performance (L/D) by increasing, relatively, induced drag coefficient while lowering, relatively, the lift coefficient. The AVL data seemed to mostly agree with other experimental data at angles of attack from 2.1 to 6.3, with the simulation growing less and less accurate as angle of attack increases. Most, if not all, of the data aligns with theory, as justified in earlier sections of the report.

References

1. Youngren, Harold, & Drela, Mark (1988). Athena Vortex Lattice [Computer software]. Retrieved January 31, 2022, from http://web.mit.edu/drela/Public/web/avl/
2. Fink, R (1960). *USAF Stability and Control DATCOM*. McDonnell Douglas Corporation, Douglas Aircraft Division, Air Force Flight Dynamics Laboratory, Wright-Patterson AFB.
3. Weber, J., and Brebner, G.G. (1958). *Low-Speed Tests on 45-deg Swept-back Wings. Part I: Pressure Measurements on Wings of Aspect Ratio 5.* Aeronautical Research Council.